Metrol. Meas. Syst., Vol. XX (2013), No. 1, pp. 53–64.

PAN POLSKA AKADEMIA NAUK

METROLOGY AND MEASUREMENT SYSTEMS

Index 330930, ISSN 0860-8229

www.metrology.pg.gda.pl

M&MS

DISTRIBUTED STRAIN RECONSTRUCTION BASED ON A FIBER BRAGG GRATING REFLECTION SPECTRUM

Małgorzata Detka, Zdzisław Kaczmarek

Kielce University of Technology, Faculty of Electrical Engineering and Measurement Systems, Aleja 1000-lecia Państwa Polskiego 7, 25-314 Kielce, Poland (✉ m.detka@tu.kielce.pl, +48 41 342 4157, z.kaczmarek@tu.kielce.pl)

Abstract

In this paper, we present a synthesis of the parameters of the fiber Bragg grating (FBG) and the reconstruction of the distributed strain affecting the grating, performed by means of its reflection spectrum. For this purpose, we applied the transition matrix method and the Nelder-Mead nonlinear optimization method. Reconstruction results of the strain profile carried out on the basis of a simulated reflection spectrum as well as measured reflection spectrum of the FBG indicate good agreement with the original strain profile; the profile reconstruction errors are within the single digit percentage range. We can conclude that the Nelder-Mead optimization method combined with the transition matrix method can be used for distributed sensing problems.

Keywords: fiber Bragg grating, synthesis, distributed sensing, transfer matrix method.

1. Introduction

Fiber Bragg gratings are commonly used as sensing elements for measuring strain, temperature and pressure. They convert these quantities to changes in the Bragg wavelength.It is assumed that the distribution of the converted quantity is uniform. Spectra of a FBG contain information on the grating parameters and thus on the distribution of the quantities affecting the grating. As a result, it is possible to reconstruct the estimates of the parameters of the FBG and the distribution of the measurand acting on it by measuring the grating spectra.

The so formulated problem becomes an inverse problem and solving it involves certain difficulties. The fact that a FBG is a nonlinear element increases the level of difficulty. Reconstructing a measurand using the grating spectra is called intra-grating sensing [1–3]. The reconstruction of the grating physical parameters is an identification problem. A number of methods have been developed to solve such problems. Some of them rely only on the measured intensity reflection spectrum [1, 2, 4–15], others depend on the phase spectrum [1, 3], and still others base on both [1, 4, 9]. They include the Fourier transform method [1, 3], the time-frequency analysis method [4], the Gelfand-Levian-Marczenko method [5], the optimization methods [6–8] the layer-peeling algorithm [9], and the genetic algorithms [10–13]. In practice, the methods based on the measured intensity spectrum of the grating are the most common because this spectrum is easy to measure. The measurement of the grating phase characteristics requires a complex and expensive measurement system, which is much more difficult to set up than it is the case with the reflection spectrum measurements.

The paper presents solutions to the inverse problems, namely the determination of the estimates of the grating parameters and the calculation of the estimates of the strain distribution along the Bragg grating, which are based on the intensity reflection spectrum of the grating. The Nelder-Mead simplex algorithm and the transition matrix method are used

Article history: received on Jul. 10, 2012; accepted on Jan. 21, 2013; available online on Mar. 15, 2013; DOI: 10.2478/mms-2013-0005.

to solve the problem. These calculations were carried out on the basis of a simulated reflection spectrum as well as a measured reflection spectrum of the FBG.

2. Reconstruction of the grating parameters and the strain distribution

The sequence of procedures in the problem posed is as follows. First, the reflection spectrum of the uniform grating for its set parameters is calculated. Next, the parameters of the grating are reconstructed on the basis of the calculated reflection spectrum, after adding noise. The next stage involves the calculation of the reflection spectrum of the grating subjected to a given strain distribution. The reconstructed parameters of the grating are used for this purpose. Finally, the strain distribution is reconstructed on the basis of the calculated spectrum with added white noise.

The reflection spectrum of a non-uniform FBG can be calculated using the matrix method [16]. The most important equations of this method will be given further in this section.

The effective refractive index of an optical fiber, which characterizes the FBG, can be described by the following function:

$$n_{eff}(z) = n_0 + \delta n_{eff}(z)\cos(\frac{2\pi}{\Lambda} z + \varphi(z)), \tag{1}$$

where n_o is the mean value of the refractive index, δn_{eff} is the amplitude of the variation of the refractive index, z is the distance along the fiber's longitudinal axis, Λ is the grating period, and $\phi(z)$ describes the grating chirp.

The grating period, whose change is caused by the strain with the profile $\varepsilon(z)$, can be expressed as:

$$\Lambda(z) = \Lambda_0[1 + (1 - p_e)\varepsilon(z)], \tag{2}$$

where Λ_0 is the initial period, and p_e is the strain-optic coefficient.

The grating apodized with a Gaussian profile can be described by the formula:

$$\delta n_{eff}(z) = \delta n_{eff} \exp\left[- \rho\left(\frac{z - L/2}{L} \right)^2 \right] = \delta n_{eff}\, g(z), \tag{3}$$

where L is the grating length and ρ is the parameter of the Gaussian function width.

The mathematical model of a FBG is a pair of coupled differential equations describing the interaction between the propagation mode with the complex amplitude $A(z)$ and an identical, counter-propagation mode with the amplitude $B(z)$:

$$\begin{aligned} \frac{dA(z)}{dz} &= j\sigma A(z) + j\kappa B(z), \\ \frac{dB(z)}{dz} &= -j\sigma B(z) - j\kappa A(z), \end{aligned} \tag{4}$$

where σ and κ are the coupling coefficients defined as:

$$\sigma = 2\pi n_{eff}\left(\frac{1}{\lambda} - \frac{1}{\lambda_B} \right) + \frac{2\pi}{\lambda}\delta n_{eff} - \frac{1}{2}\frac{d\phi}{dz}, \qquad \kappa = \frac{\pi}{\lambda}\delta n_{eff}\, g(z), \tag{5}$$

where λ_B is the Bragg wavelength $\lambda_B = 2n_{eff}\Lambda$.

In order to obtain solutions to (4), the grating is divided into M uniform sections. In each section with the length Δz, the coefficients σ and κ are constant. The light wave propagation through each section k ($k = 1,\ldots M$) is described by the equation:

$$\begin{bmatrix} A_k \\ B_k \end{bmatrix} = T_k \begin{bmatrix} A_{k-1} \\ B_{k-1} \end{bmatrix}, \tag{6}$$

where A_k, B_k are amplitudes of the light waves after the transition of the k-th section; the transition matrix T_k takes the form:

$$T_k = \begin{bmatrix} \cosh(\gamma dz) - j\frac{\sigma}{\gamma}\sinh(\gamma dz) & -j\frac{\kappa}{\gamma}\sinh(\gamma dz) \\ j\frac{\kappa}{\gamma}\sinh(\gamma dz) & \cosh(\gamma dz) + j\frac{\sigma}{\gamma}\sinh(\gamma dz) \end{bmatrix}, \tag{7}$$

where $\gamma = \sqrt{\kappa^2 - \sigma^2}$.

The total grating structure can be described by the matrix T, which is the product of the transition matrices of all sections:

$$T = T_M \cdot T_{M-1} \cdot \ldots \cdot T_k \cdot \ldots \cdot T_1 = \begin{bmatrix} t_{11} & t_{12} \\ t_{21} & t_{22} \end{bmatrix}. \tag{8}$$

The spectrum of the beam reflected by the grating is calculated taking into account the boundary conditions $A_0 = 1$, $B_0 = 0$.

The power reflection coefficient for the whole grating takes on the form:

$$R = \left| -\frac{t_{21}}{t_{22}} \right|^2. \tag{9}$$

From the above relationships, it is possible to calculate the reflection spectrum of the FBG for the given parameters L, Λ, δn_{eff}, ρ and $\varepsilon(z)$.

The reconstruction of the strain profile and the synthesis of the grating are performed using one of the optimization techniques, *i.e*. the Nelder-Mead simplex method. In an n-dimensional space, that is when n parameters have to be reconstructed, a simplex is a geometric figure that has $n + 1$ vertices. The Nelder-Mead method involves the transformation of the simplex selected at the beginning of the calculations x_i (i = 1,…,n + 1) in such a way that its worst point (the highest value of the objective function) is replaced with a new, better point. Decisions on a new location of the simplex vertices are made on the basis of the values of the objective function at the current points. The transformation of the simplex is continued until the distance between its vertices in the vicinity of the minimum sought is not greater than the assumed accuracy. The initial simplex is constructed around a given starting point x_0 by changing individual coordinates by 10%. The mean square deviation between the modeled and the reconstructed spectra of the grating is assumed to be the objective function:

$$f(\alpha) = \sqrt[4]{\left(\int_0^\infty \left[R_{mod}(\lambda) - R_{rec}(\lambda, \alpha_1, ..., \alpha_n)\right]^4\right) d\lambda}, \tag{10}$$

where $R_{mod}(\lambda)$ and $R_{rec}(\lambda,\alpha_1,\ldots,\alpha_n)$ are the modeled and the reconstructed spectra of the grating, respectively. The optimal values of parameters α_1,..., α_n are obtained by determining the minimum of the objective function $f(\alpha)$. The diagram illustrating the optimization stages is shown in Fig. 1.

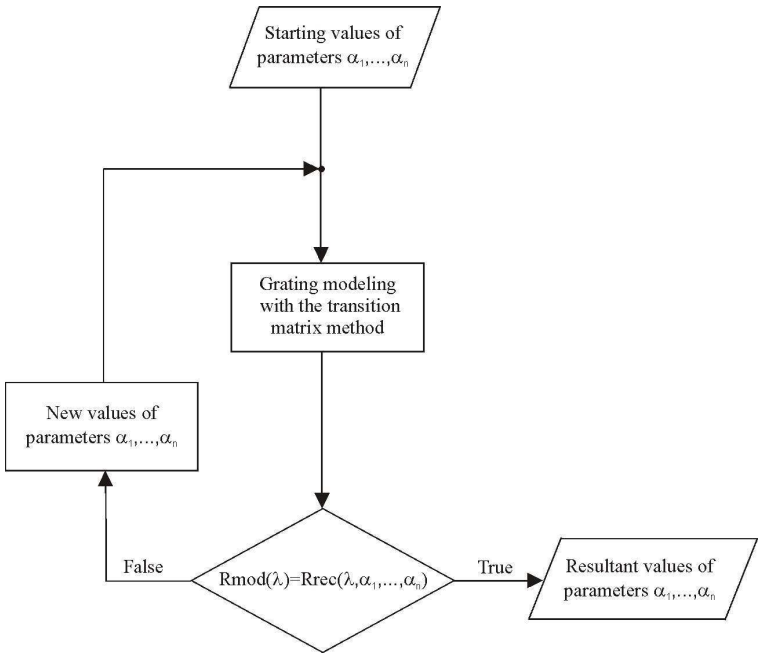

Fig. 1. Diagram showing the stages of the optimization procedure.

A detailed description of the Nelder-Mead method can be found in [17].

3. Results of the simulation

First, the parameters of the unstrained grating are reconstructed. The FBG is characterized by the following parameters: L, Λ, δn_{eff}, and ρ. The reflection spectrum of the grating is then calculated for the assumed values of the grating parameters shown in Table 1 and apodized with a Gaussian function according to (3), using the transition matrix method. The calculated spectrum is presented in Fig. 2. The spectral resolution of the simulation is set at 0.01 pm. White noise is added to the calculated spectrum. For the sake of the simulation, the grating is divided into fifty equal sections. On the basis of the calculated reflection spectrum, the reconstruction of the grating parameters is performed using the Nelder-Mead simplex algorithm with the objective function, in accordance with (10), where it is assumed that $\alpha_1 = L$, $\alpha_2 = \Lambda$, $\alpha_3 = \delta n_{eff}$, $\alpha_4 = \rho$. The optimization procedure is performed as shown in the diagram in Fig. 1. The values of the parameters with a 40% deviation from the original ones are assumed to be the starting values of the reconstructed parameters. The results of the reconstruction of the grating parameters, together with the reconstruction errors, are presented in Table 1.

Table 1. Reconstruction results of the physical parameters of the FBG.

Parameters	**Original values**	**Reconstructed values**	**Maximum relative error**
L (mm)	10	9.963	3.7×10^{-3}
Λ (nm)	530.834	530.833998	3.9×10^{-7}
δn_{eff} (10^{-5})	26	25.880	4.6×10^{-3}
ρ	0.5	0.481	3.9×10^{-2}

The calculations indicate that the parameters L, δn_{eff} are reconstructed with an error not greater than 0.5%, whereas the grating period Λ is reconstructed very accurately because the error does not exceed $4 \cdot 10^{-5}$%. The value of the parameter of the apodization function ρ is reconstructed least accurately; here, the reconstruction error amounts to 3.9%. On the basis of the reconstructed parameters of the grating, the reflection spectrum is calculated. Fig. 2 presents the grating reflection spectra, *i.e.* the original one and that calculated from the reconstruction. The agreement between the shapes of the spectra is very good, which results from the exact reconstruction of the grating parameters.

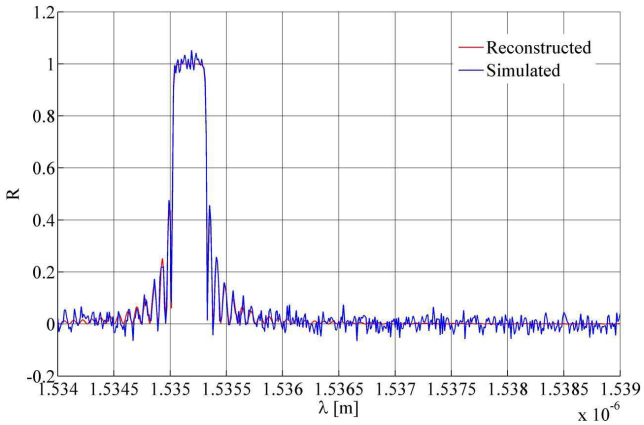

Fig. 2. Simulated reflection spectrum with 2.5% noise and reconstructed reflection spectrum of the grating.

The next step involves the reconstruction of the strain distribution, which is performed on the basis of the modeled spectrum, generated by the original strain distribution. It is assumed that the strain distribution is a first order function: $\varepsilon(z) = a_1 + a_2 z$. Once the grating parameters L, Λ, δn_{eff} and ρ are determined in the first stage, a_1 and a_2 become the unknown parameters. Like in the first stage, the proposed method can be employed to determine the values of the two parameters and, accordingly, to reconstruct the strain distribution $\varepsilon(z)$.

At this stage of the reconstruction, the assumed parameters of the grating are as follows $L = 10$mm, $\Lambda = 530.834$ nm, $\delta n_{eff} = 26 \cdot 10^{-5}$ and $\rho = 0.5$. The grating is also divided into fifty sections ($M = 50$). Fig. 3 shows the simulated strain profile and the reconstructed strain profile for two different pairs of the parameters a_1 and a_2. The results of the errors of the reconstruction of the strain profile are presented in Table 2. From the table it is clear that the reconstruction error for the strain (parameter a_1) is less than 0.1%, whereas the reconstruction error for the strain gradient (parameter a_2) does not exceed 1.5%. The spatial resolution of the reconstructed strain profile, which is 0.2 mm, results from the assumed number of FBG sections in the transition matrix method.

Table 2. Errors of the reconstruction of the strain profile.

$\varepsilon(z)$	Reconstructed values of the strain polynomial coefficient		Strain error a_1[%]	Gradient error a_2[%]
	a_1[με]	a_2[με/mm]		
1209με+(13.44με/mm)z	1210.27	13.63	0.056	1.40
2419με+(26.88 με/mm)z	2421.04	27.20	0.076	1.21

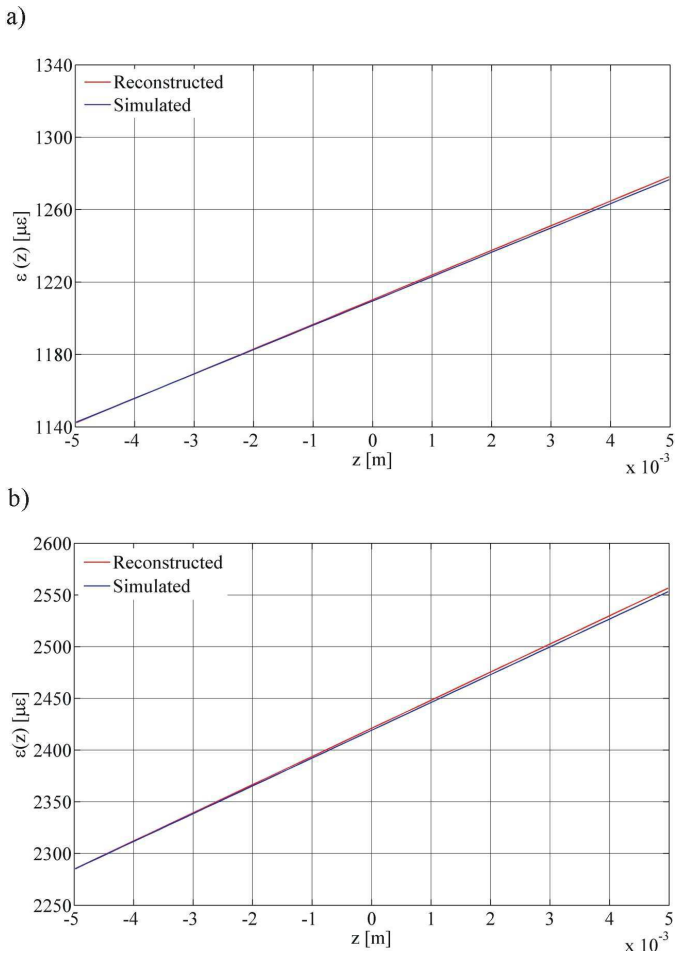

Fig. 3. Simulated strain profile and reconstructed strain profile: a) $\varepsilon(z) = 1209\mu\varepsilon + (13.44\mu\varepsilon/\text{mm})z$; b) $\varepsilon(z) = 2419\mu\varepsilon + (26.88\ \mu\varepsilon/\text{mm})z$.

The simulated reflection spectrum and the reconstructed reflection spectrum of the grating subjected to distributed strain $\varepsilon(z) = a_1 + a_2 z$ for two pairs of the parameters a_1 and a_2 is shown in Fig. 4. It can be seen that the shapes of these spectra, as well as their central wavelengths, are almost identical. Moreover, it can be noticed that the strain with the linear profile (*i.e.* the strain with the constant gradient) broadens the reflection spectrum and reduces the peak reflectivity. The relative 3 dB bandwidth of the grating is linearly dependent on the strain gradient in the range 0–26.88 με/mm. A reduction in the peak reflectivity is observed for the strain gradient above 25 με/mm. These results are consistent with the experimental results published in [18–20].

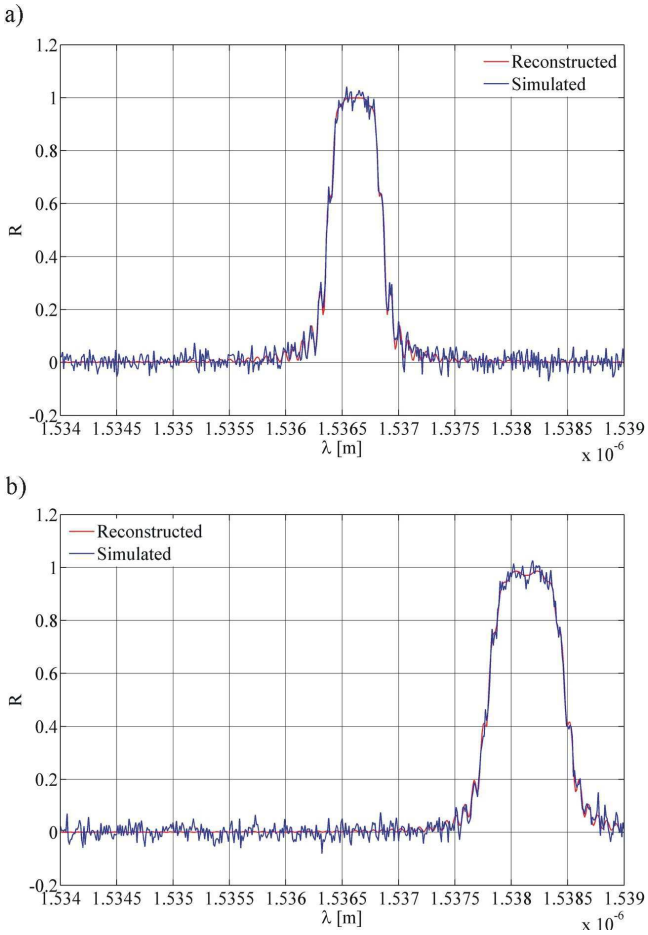

Fig. 4. Simulated reflection spectrum and reconstructed reflection spectrum of the grating for the strain profile: a) $\varepsilon(z) = 1209\mu\varepsilon+(13.44\mu\varepsilon/\text{mm})z$; b) $\varepsilon(z) = 2419\mu\varepsilon+(26.88\ \mu\varepsilon/\text{mm})z$.

4. Reconstruction results based on the the measured spectrum

Like in the simulation, we began with a synthesis of the parameters of the measured grating based on the measured reflection spectrum of the unstrained grating. Then, using these parameters and the measured reflection spectrum of the grating subjected to distributed strain, we applied the Nelder-Mead optimization procedure to reconstruct the strain profile. The measurements of the reflection spectrum of the unstrained fiber Bragg grating as well as the grating subjected to distributed strain were performed using a measuring setup described in [18]. The spectral resolution of the measurement of the reflection spectrum was equal to 5 pm at the wavelength range of 5 nm. The measurements were conducted for a cantilever beam with a FBG installed on it. The beam was subjected to a load at the free end. The distributed strain produced in the beam can be expressed in the form of a strain with a constant gradient. This distributed strain acting along the grating can be written as:

$$\varepsilon(z) = \varepsilon + \frac{d\varepsilon}{dz} z\,, \tag{11}$$

The strain ε and the strain gradient $d\varepsilon/dz$ are linearly dependent on the beam deflection. The measurement results were used to reconstruct the strain profiles. According to the specifications provided by the producer, the grating length was 10 mm. Thus, the parameters to be reconstructed were: $\alpha_1 = \Lambda$, $\alpha_2 = \delta n_{ef}$, $\alpha_3 = \rho$. Their values were determined using the measured reflection spectrum of the unstrained grating. The reconstruction results are given in Table 3.

Table 3. Reconstruction results of the physical parameters of the FBG.

Parameters	Reconstructed values
Λ (nm)	530.836
δn_{eff} (10^{-5})	259.329
ρ	0.3606

Using the reconstructed parameters of the grating, we calculated its reflection spectrum. Fig. 5 presents the measured spectrum and reconstructed spectrum of the grating. It can be seen that there is good agreement between the shapes of these spectra and their central wavelengths.

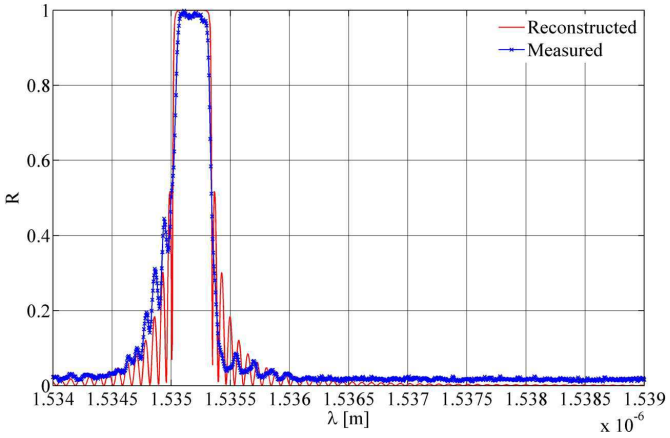

Fig. 5. Measured reflection spectrum and reconstructed reflection spectrum of the grating.

Subsequently, knowing the grating parameters and the measured reflection spectrum of the grating subjected to distributed strain, we performed calculations to reconstruct the parameters of the distributed strain. Fig. 6 shows the reconstructed strain distribution toghether with the corresponding distribution determined from the relationships assumed for a cantilever beam being deflected. The following well-known relationship for a deflected cantilever beam strain was used:

$$\varepsilon = \frac{3hl}{2l_0^3} f, \tag{12}$$

where: f, l_0, h, l are the deflection, length and thickness of the beam, and l is the distance from the free end of the beam.

If one relates the axial coordinate of the beam l and the axial coordinate of the grating to the expression $l = l_c + z$, where l_c is the distance of the center of the grating, mounted on the beam, from the free end of the beam, then on the basis of relation (12) the terms of the right side of formula (11) are given by the relations:

$$\varepsilon = \frac{3hl_c}{2l_0^3} f \quad \text{and} \quad \frac{d\varepsilon}{dz} = \frac{3h}{2l_0^3} f, \tag{13}$$

where ε is the strain of the center of the grating.

Assuming that the values of the parameters of the distributed strain, ε and $d\varepsilon/dz$, determined from relationships (13) were the reference values, we calculated the maximum relative errors of the reconstruction of these parameters, which are given in Table 4. From the table we can see that the the error of the reconstruction of the strain is less than 0.5%, while the error of the reconstruction of the strain gradient does not exceed 3.0%.

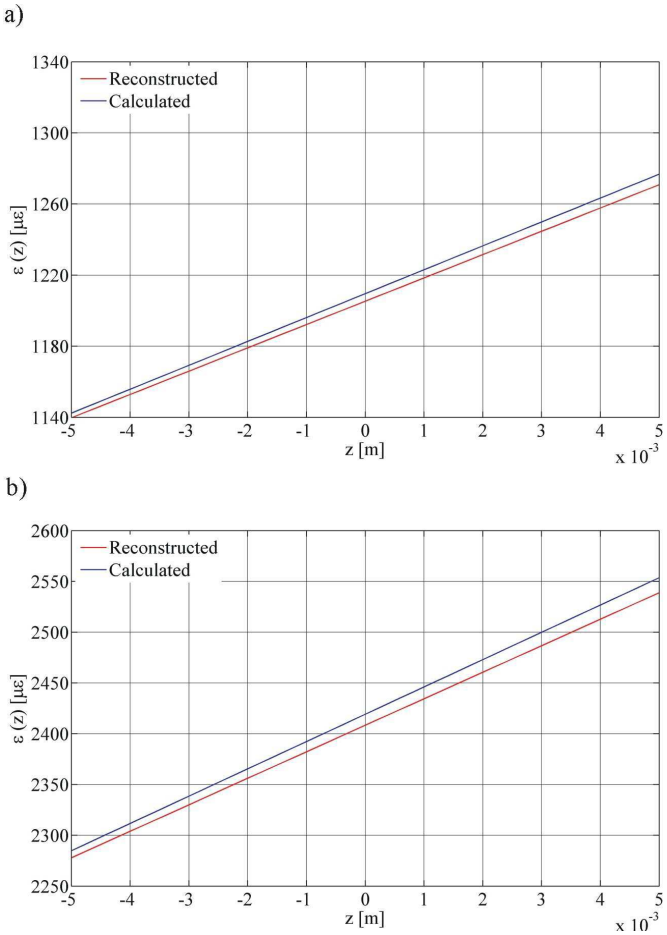

Fig. 6. Calculated strain profile and reconstructed strain profile: a) $\varepsilon(z) = 1209\mu\varepsilon + (13.44\mu\varepsilon/\text{mm})z$; b) $\varepsilon(z) = 2419\mu\varepsilon + (26.88\ \mu\varepsilon/\text{mm})z$.

Table 4. Errors of the reconstruction of the strain profiles.

Calculated values of the strain polynomial coefficient		**Reconstructed values of the strain polynomial coefficient**		**Strain error a_1[%]**	**Gradient error a_2[%]**
a_1[με]	**a_2[με/mm]**	**a_1[με]**	**a_2[με/mm]**		
1209.6	13.44	1205.33	13.11	0.35	2.45
2419.2	26.88	2408.34	26.10	0.45	2.92

Figure 7 presents the measured reflection spectrum and the reconstructed reflection spectrum of the fiber Bragg grating subjected to the strain distribution $\varepsilon(z) = \varepsilon + (d\varepsilon/dz)z$ for two different pairs of the parameters a_1 and a_2. We can see that there is good agreement between the shapes of these spectra as well as their central wavelengths.

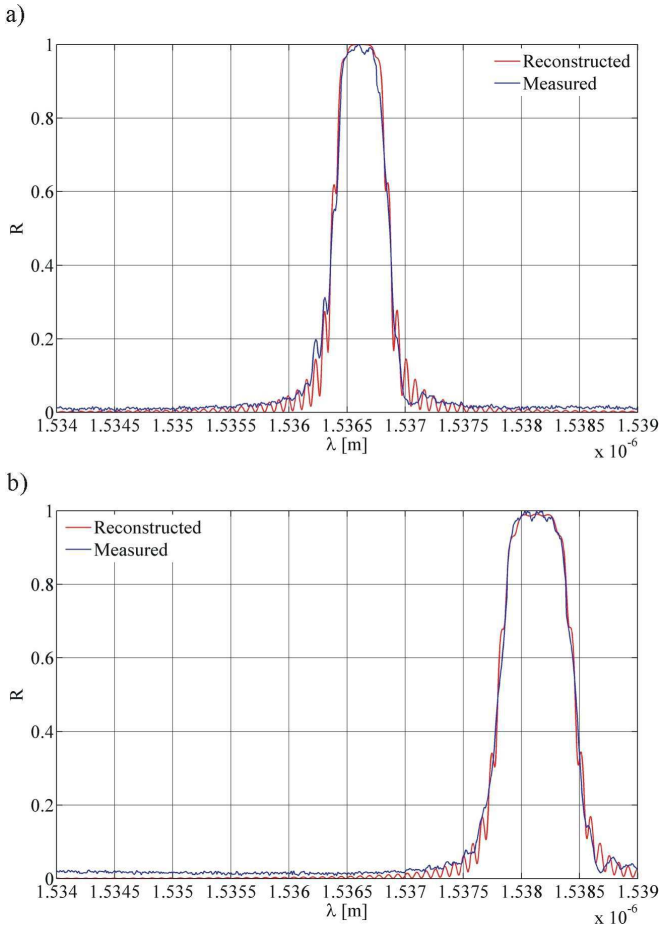

Fig. 7. Measured reflection spectrum and reconstructed reflection spectrum of the grating for strain profile: a) $\varepsilon(z) = 1209\mu\varepsilon + (13.44\mu\varepsilon/\text{mm})z$; b) $\varepsilon(z) = 2419\mu\varepsilon + (26.88\ \mu\varepsilon/\text{mm})z$.

5. Conclusions

In the study, we applied the Nelder-Mead simplex algorithm and the transition matrix method to synthesize the parameters of the fiber Bragg grating and reconstruct the strain

profile along the grating length by using the grating reflection spectrum. The simulation calculations showed that the synthesis of the grating parameters was performed with an error not exceeding 0.5%, whereas the reconstruction of the strain profile was conducted with an error less than 1.5%. The error of the reconstruction of the strain profile based on the measured reflection spectrum was less than 3%.

The spatial resolution of the reconstructed strain profile is determined by the number of sections of the fiber Bragg grating assumed in the transition matrix method, which was 0.2 mm. The reconstruction results of the strain profiles carried out on the basis of the simulated reflection spectrum and the measured reflection spectrum of the FBG indicate that the Nelder-Mead algorithm combined with the transition matrix method can be successfully used for distributed sensing problems.

Acknowledgements

This work was supported by the European Regional Development Fund, contract no. POIG.02.02.00-26-023/09.

References

[1] Othonos T.A., Kalli, K. (1999). *Fiber Bragg Grating: Fundamentals and Applications in Telecommunications and Sensing.* Artech House, Boston, London.

[2] Hung , S., Leblanc, M., Ohn, M.M., Measures R. M. (1995). Bragg intragrating structural sensing. *Appl Opt.*, 34(22), 5003–5009.

[3] Hung, S., Ohn, M.M., Measures, R.M. (1996). Phase-based Bragg intragrating distributed strain sensor. *Appl. Opt.*, 35(7), 1135–1142.

[4] Azana, J., Muriel, M.M., Chen, L.R., Smith, P.W. E. (2001). Fiber Bragg grating period reconstruction using time-frequency signal analysis and application to distributed sensing. *J. Lightwave Technol.*, 19(5), 646–654.

[5] Peral, E., Capmany, J., Marti, J. (1996). Iterative solution to the Gel'Fand-Levitan-Marchenko coupled equations and application to synthesis of fiber gratings. *IEEE J. Quantum Electron.*, 32, 2078–2084.

[6] Shi, C., Zeng, N., Zhang, M., Liao, Y., Lai, S. (2003). Adaptive simulated annealing algorithm for the fiber Bragg grating distributed strain sensing. *Opt. Commun.*, 226, 167–173.

[7] Li, M., Zeng, N, Shi, C., Zhang, M,. Liao, Y. (2005). Fiber Bragg grating distributed strain sensing: an adaptive simulated annealing algorithm approach. *Optics & Laser Technol.*, 37, 454–457.

[8] Zou, H., Liang, D., Zeng, J., Feng, L. (2012). Quantum-behaved particle swarm optimization algorithm for the reconstruction of fiber Bragg grating sensor strain profiles. *Opt. Commun.*, 285, 539–545.

[9] Skaar, J., Wang, L., Erdogan, T. (2001). On the synthesis of fiber Bragg gratings by Layer Peeling. *IEEE J. Quantum Electron.*, 37, 165–173.

[10] Casagrande, F., Crespi, P., Grassi, A.M., Lulli, A., Kenny, R.P., Whelan, M.P. (2002). From the Reflected Spectrum to the Properties of a Fiber Bragg Grating: A Genetic Algorithm Approach with Application to Distributed Strain Sensing. *Appl Opt.*, 41(25), 5238–5244.

[11] Cheng, H.Ch., Huang, J.F, Chen, Y.H. (2008). Reconstruction of phase-shifted fiber Bragg grating parameters using genetic algorithm over thermally-modulated reflection intensity spectra. *Optical Fiber Technology*, 14, 27–35.

[12] Zhang, R., Zheng, S., Xia, Y. (2008). Strain profile reconstruction of fiber Bragg grating with gradient using chaos genetic algorithm and modified transfer matrix formulation. *Opt. Commun.*, 281, 3476–3485.

[13] Gill, A., Peters, K., Studer, M. (2004). Genetic algorithm for the reconstruction of Bragg grating sensor strain profiles. *Meas. Sci. Technol.*, 15, 1877–1884.

[14] LeBlanc, M., Huang, S.Y., Ohn, M.M., Measures, R.M.,A., Guemes, Othonos, A. (1996). Distributed strain measurement based on a fiber Bragg grating and its reflection spectrum analysis. *Opt. Lett.*, 21, 1405–1407.

[15] Hung, S., Ohn, M.M., Leblanc, M., Measures, R.M. (1998). Continuous arbitrary strain profile measurements with fiber Bragg gratings. *Smart Materials and Structures*, 7, 248–256.

[16] Erdogan, T. (1997). Fiber grating spectra. *J. Lightwave Technol.*, 15(8), 1277–1294.

[17] Lagaris, J.C., Reeds, J.A. Wright, M.H., Wright, P.E. (1998). Convergence Properties of the Nelder-Mead Simplex Method in Low Dimensions. *Siam J. Optimizat.*, 9(1), 112–147.

[18] Kaczmarek, Z., Detka, M. (2010). Influence of the strain gradient of a uniform fiber grating on its spectral characteristics. *Measurement Automation and Monitoring*, 12, 1439–1441.

[19] Prabhugoud, M., Peters, K. (2004). Modified transfer matrix formulation for Bragg grating strain sensors. *J. Lightwave Technol.*, 22(10), 2302–2309.

[20] Peters, K., Pattis, P., Botsis, J., Giaccari, P. (2000). Experimental verification of respone of embedded optical fiber Bragg grating sensors in non-homogeneous strain fields. *Optics & Lasers Engineering*, 33, 107–119.